Int. J. Nano Dimens., 13 (4): 387-396, Autumn 2022

ORIGINAL ARTICLE

Preparation and investigation of M-MWCNT nanocomposite by hydrothermal method for Pb(II) ions adsorption

Mojtaba Zabihi[1], Alireza Motavalizadehkakhky[2,3,], Maryam Omidvar[4,*], Rahele Zhiani[2,5], Seyed Mohammad Mahdi Nouri[6], Hamid Heydarzadeh Darzi[6]*

[1] *Department of Chemical Engineering, Neyshabur Branch, Islamic Azad University, Neyshabur, Iran*
[2] *Department of Chemistry, Neyshabur Branch, Islamic Azad University, Neyshabur, Iran*
[3] *Avdanced Research Center of Chemistry Biochemistry & Nanomaterial, Neyshabur Branch, Islamic Azad University, Neyshabur, Iran*
[4] *Department of Chemical Engineering, Quchan Branch, Islamic Azad University, Quchan, Iran*
[5] *New Materials Technology and Processing Research Center, Department of Chemistry, Neyshabur Branch,Islamic Azad University, Neyshabur, Iran*
[6] *Chemical Engineering Department, Hakim Sabzevari University, Sabzevar, Iran*

Received 15 June 2022; revised 27 July 2022; accepted 29 July 2022; available online 03 August 2022

Abstract

In this present work, MWCNTs modified $NiFe_2O_4$ NPs (M-MWCNT) were successfully fabricated based on a hydrothermal route, and then utilized to Pb(II) sorption from an aqueous solution. The M-MWCNT was characterized and analyzed by SEM, TEM, FTIR, XRD, and VSM techniques. TEM image demonstrated that the size of NiFe2O4 nanoparticles in the structure of MWCNT was 20 nm. VSM results indicated that the M-MWCNT with saturation magnetization (Ms) value of 7 emu/g would have a fast magnetic response. According to X-ray data the average crystal sizes of the pure NiFe2O4 and M-MWCNT are 21.62 and 7.25 nm, respectively. The sorption kinetics, isotherms, thermodynamic and regeneration performance for lead ((Pb(II)) ions were evaluated. The M-MWCNT can effectively remove Pb(II) from aqueous solution at optimum pH of 5.5. Based on the Langmuir model, the maximum saturated adsorbed amount (qmax) of Pb(II) was up to 85.12 mg/g. The kinetic characteristic was appropriate for pseudo 1st order model expression, and the isothermal characteristic can be described via Longmuir model. The data obtained from the thermodynamic study show that the Pb(II) sorption using M-MWCNT nanocomposite was a spontaneous, exothermic and physisorption process with a good regeneration performance.

Keywords: *Isotherms; Kinetics; MWCNT; Nanocomposite; $NiFe_2O_4$ NPs; Pb(II) Sorption; QMAX.*

How to cite this article

Zabihi M., Motavalizadehkakhky A., Omidvar M., Zhiani R. ,Nouri S.M.M., Heydarzadeh Darzi H. Preparation and investigation of M-MWCNT nanocomposite by hydrothermal method for Pb(II) ions adsorption. Int. J. Nano Dimens., 2022; 13(4): 387-396.

INTRODUCTION

The control and removal of toxic components from water such as heavy metal ions, dyestuff waste, pesticides, pharmaceutical waste, and bacteriological contamination constitute a vital research domain [1]. Lead (Pb) is one of the common heavy metal contaminants in wastewater, specifically in battery industrial wastewater. The release of Pb in the environment could lead to human health issues [2].

According to the World Health Organization reportes accures 143 million deaths due to Pb(II) pollutants in the developing countries annually. Hence, the permissible limit is 0.05 mg/L set by the US Environmental Protection Agency and 0.01 mg/L, which is regulated by the EU countries [3]. A high number of research works have been carried out on the adsorptive removal of PB(II)

* Corresponding Author Email: amotavalizadeh@yahoo.com
omidvar_qu@yahoo.com

metal ions. Abdel-Ghani *et al.* were employed low-cost adsorbents such as rice husks, maize cobs and sawdust for removal of Pb(II) at different adsorbent/metal ion ratios. They found that the sorption efficiencies were found to be pH dependent, rising by enhancing the solution pH from 2.5 to 6.5. they work results indicated the maximum removal percentage was obtained at an adsorbent dosage of 1.5 g in the equilibrium time of 120 min. Also, it was illustrated that Temkin isotherm model had best fitted the adsorption data [4].

Plenty of adsorbents, like activated carbon, graphene oxide, nano-materials, biomaterials, polymeric material, MOFs, and Carbon nanotubes (CNTs) have been utilized for the removal of Pb from water.

CNTs have a promising future as sorbent for the removal of different pollutants from wastewater. Multi-wall carbon nanotubes possess some favorable attributes of tiny size and diameter, layered hollow skeleton, enormous surface area, high aspect ratio, and good mechanical strength and conductivity [5, 6]. Nonetheless, MWCNTs nanocomposite could not be easily separated from the liquid phase via filtration or centrifugation owing to their nano size and low density. The uncontrolled discharge of MWCNTs in the environment is a trouble due to their natural and ecological damages. Thus, the fabrication of an MWCNTs nanocomposite with easily separable is critical to its wide application in the future [7].

For increasing the separation of MWCNTs from the treated solution, it could be modified using magnetic NPs like Fe_2O_3, Fe_3O_4, $CoFe_2O_4$, $MnFe_2O_4$ and $NiFe_2O_4$ as an effective and non-contact method [8]. Magnetic adsorbents have attracted plenty of attention from researchers in wastewater treatment processes [7, 9-11]. In special, $NiFe_2O_4$ with high density, high saturation magnetization, moderately enormous surface area, good thermal stability, and acid resistance is an excellent candidate to be applied in wastewater treatment [12]. Many researchs have been carried out on the adsorptive removal of pullutant using magnetic NPs. For example, Hakimyfard and Khademinia [13] findings indicated that the optimized conditions for the degradation of a 100 mL of 80 ppm MG aqueous solution by $NiFe_2O_4$ are 0.03 mL H_2O_2, 0.038 g catalyst and 45 min reaction time. The degradation yield at the optimized conditions under visible light irradiation was 95 %. The light source was a white color fluorescent lamp with the 40 W power and light intensity of 1.34 W/m^2 measured by a digital lux meter. Bagheri *et al.* [14] successfully used $CuFe_2O_4$ in the photodegradation of acid red 206 from aqueous solution. The results show that the $CuFe_2O_4$ is an active photocatalyst. A first order reaction with K=0.123 min^{-1} was observed. Abideen Idowu *et al.*[15] showed that adsorption of digestive enzymes was hardly adsorbed by $MnFe_2O_4$ sorbent. The sorption was study in a batch system and the data were subjected to isotherm and kinetics models. The pseudo 1st order model best fitted the kinetic data with R^2> 0.99. The data were fitted well by the entire isotherm models considered with the maximum adsorption uptake of 1.602 and 7.330 mg/g. Decoration of MWCNTs surface by spinel ferrite NPs could lead to boosting optical, magnetic, and electrochemical properties of MWCNTs [16]. Kafshgari *et al.* [17] have synthesized $MnFe_2O_4$/MWCNT to adsorb DR16 (607.79 mg/g) and Y40 dyes (280 mg/g) from aqueous solution. Foroutan *et al.* [18] successfully used CNT/MgO/$CuFe_2O_4$ magnetic composite for adsorption of methyl violet (36.46 mg/g) and Nile blue (35.60 mg/g) from aqueous solution. The adsorption capacities of dyes by CNT adsorbents have been extensively reviewed by Sadegh *et al.* [19].

In this work, a novel sorbent $NiFe_2O_4$@ MWCNTs employs to adsorb Pb(II). Properties of multiwall carbon nanotubes decorated $NiFe_2O_4$ NPs (M-MWCNTs) were evaluated with different methods such as SEM, TEM, XRD, FTIR, and VSM. In the next step, the removal percentage of lead ions was assessed and isotherm, kinetics, and thermodynamics of adsorption were examined. In view of the sorption results and reuse ability of the M-MWCNT nanoadsorbent, the M-MWCNT has been suggested as a highly promising adsorbent for useful application in the water treatment industry.

EXPERIMENTAL SECTION

Materials and apparatus

The MWCNTs (95% purity) were purchased from US Research Nanomaterials, Inc. All other chemicals used in this study ($Ni(NO_3)_2{\cdot}6H_2O$, $Fe(NO_3)_3{\cdot}9H_2O$, $Pb(NO_3)_2$, HCl and NaOH) were bought from Merck.

Fabrication of M-MWCNTs nanocomposite

The M-MWCNTs nanocomposites were fabricated via the hydrothermal route. Briefly, 200 mg MWCNT was dispersed into a 50 mL double distilled water to obtained a homogenous solution. Then, a solution of 1M Ni $(NO_3)_2$ and 2M Fe $(NO_3)_3$ was added to the aforementioned mixture. A few drops of NaOH solution (2 M) were gently added under constant mechanical stirring for adjusting the pH of the solution (pH=12). Afterward, the suspension was stirring at 40 °C for 2 hours in a hot bath. Then the homogenous suspension shifted to autoclave (Teflon lined) and heated at 160 °C in an electric oven and kept at this temperature for 15 hours. To remove impurities (e.g., NO_3^- and Na^+), obtained product was rinsed using double distilled water several times and subsequently the M-MWCNTs nanocomposite were separated from the liquid phase by a magnet. At the end, the nanocomposites were dried in an electric oven at 100 ± 5 °C for 8 hours. The fabricated M-MWCNT adsorbent was stored in a desiccator before use [6, 8, 20].

Characterization techniques

The synthesized nanocomposite was assessed by a SEM (Sigma, Carl Zeiss, and Germany) and a TEM (Zeiss-EM10C). The TEM was used to achieved images at an acceleration voltage of 80 kV. A X'pert MPD, Philips diffraction spectrometer with Cu Kα radiation (λ = 1.54 Å) was utilized to measure the X-ray diffraction. FTIR spectroscopy was utilized to detect the functional group of the fabricated M-MWCNTs from 400 to 4000 cm^{-1} a Bruker-VEATOR22. The magnetic properties were obtained by a VSM (MDKFD, Meghnatis Daghigh Kavir. Co, Iran) at ambient temperature. The zeta potential of the nanocomposite suspension was measured by MICROTRAC Nanotrac Wave particle size analyzer.

Adsorption measurements

Batch experiments were used to carry Pb(II) removal measurements in 100 mL conical flasks using a horizontal shaker with a shaking speed of 200 rpm. The sorption kinetics, isotherm, and the impact of pH on Pb(II) sorption by the M-MWCNTs were performed. To study the kinetic and isotherm of sorption, tests at various shaking times (2-210 minutes) and various Pb(II) concentrations (20-150 ppm) were implemented, respectively. The solution was shaken continuously at 200 rpm in a temperature varying from 298 to 318 ºK. At the end of experiments, the solid and liquid phases were separated by a magnet and final Pb(II) concentration was determined by Thermo Elemental's SOLAAR S Series atomic absorption spectrometry [21].

For investigation impact of pH, a predetermined dose of M-MWCNTs was added into the vials containing a specified initial concentration of Pb(II) at pH value from 2.0 to 6.0 (setting with addition of hydrochloric acid 0.1 mol/L) at ambient temperature. It is proven that the acidic conditions, lead is the majority generally located as ions in +2 oxidation form. Pb(II) ions hydrolyze in the aquatic phase at a pH over 5.5, depending on their concentration. At pH value above 6, complexes of Pb(II) such as $Pb(OH)_3^-$, $Pb(OH)_2$, $Pb_3(OH)_4^{3+}$, and $Pb_4(OH)_4^{4+}$ are constituted in the liquid medium and this indicates that the Pb(II) sorption is mostly due to precipitation but not sorption [22-25].

In the elution sorption recycle test, hydrochloric acid (2 M) was applied as a desorption agent. First, a mixture of HCl with M-MWCNT adsorbed Pb(II) was reacted for 8 hours at 298 ºK. Next, the adsorbent can readily be eliminated from solution using a magnetic field. Subsequently, the regenerated adsorbent was eluted with double distilled water (to remove the adsorbed acid) and again reused for adsorption of Pb ions. Four lead adsorption-desorption regeneration tests were conducted on the M-MWCNT sorbent. Each experiment was repeated in triplicates, and the average magnitudes were selected for further analysis, the relative error of the outcomes was less than 1%.

Calculations

The uptake capacity and removal percentage are formulated by the fallowing Eqs. (1) and (2) [26]:

$$q_t = \frac{(C_0 - C_t)V}{m} \quad (1)$$

$$R(\%) = \frac{C_0 - C_t}{C_0} \times 100 \quad (2)$$

in which q_t(mg/g): the uptake capacity, C_0(ppm): initial concentration, C_t(ppm): concentration at time t, and R (%): removal percentage.

To assess the sorption kinetics, two reaction kinetic models were used: the Lagergren pseudo 1st order (LFO) expressed by Eq. (3), and the Ho-McKay's pseudo 2nd order (PSO) expressed by Eq. (4) [17]:

$$\ln(q_e - q_t) = \ln q_e - k_1 t, \quad (3)$$

in which q_e and q_t (mg/g) denote amounts of dye adsorbed at equilibrium and time t, respectively, and k_1 (1/min) refers to the rate constant of the LFO.

$$\frac{t}{q_t} = \frac{1}{k_2 q_e^2} + \frac{t}{q_e} \quad (4)$$

in which k_2 (g/(mg min)) is the rate constant of the PSO.

The sorption experiments were also fitted by the Langmuir and Freundlich sorption isotherms according to Eqs. (5) and (6), respectively [17].

$$q_e = \frac{q_m k_l C_e}{1 + k_l C_e} \quad (5)$$

$$q_e = k_F C_e^{\frac{1}{n_f}} \quad (6)$$

in which q_m (mg/g) indicates the maximum sorption capacity and k_l (L/g) is the Langmuir constant illustrating the binding site affinity. In addition, k_F (L/g) is Freundlich constant representing the sorption capacity.

To evaluated the impact of temperature on sorption of Pb(II), sorption tests were also performed at 298, 308 and 318 K. The thermodynamic parameters like change of enthalpy (ΔH°, J/mol), entropy (ΔS°, J/mol K) and Gibbs free energy (ΔG°, J/mol) magnitudes were estimated from the linearized Van't Hoff equation, Eqs. (7) and (8) [27]:

$$\Delta G^\circ = -RT \ln K_c \quad (7)$$

$$\ln K_c = \frac{\Delta S^\circ}{R} - \frac{\Delta H^\circ}{RT} \quad (8)$$

where K_c is the adsorption equilibrium constant (L/g), R and T represent the universal gas constant (8.314 J/mol K) and the Kelvin, respectively.

RESULTS AND DISCUSSIONS

Characterization of M-MWCNTs nanocomposites

The surface morphology of the as-prepared $NiFe_2O_4$ NPs and M-MWCNT nanocomposite were illustrated by SEM, as observed in Figs. 1(a) and 1(b). In Fig. 1(a), particles that are spherical in shape with extremely small in dimension are evident in the SEM picture, and represented the regular morphology of $NiFe_2O_4$ NPs. Also, Fig. 1(b) reveals that $NiFe_2O_4$ NPs are successfully decorated on the outer walls of MWCNTs using covalent modified.

Moreover, extra investigation of morphology and building of M-MWCNT was taken out using the TEM technique. The TEM image of the as-mentioned specimen is depicted in Fig. 1(c). TEM image demonstrated that the size of $NiFe_2O_4$ nanoparticles in the structure of MWCNT was 20 nm.

FTIR technique provides good information about the dominant functional groups and the characteristic vibrational bands of samples. Fig. 1(d) revealed FTIR pattern of samples. The presence of peak at 3500 cm^{-1} is ascribed to stretching vibration of OH adsorbed on the surface of samples. The absorbance around 2900 cm^{-1} is corresponded to $–CH_3/CH_2$ stretching vibration and the peak at 1400-1600 cm^{-1} was attributed to C=O stretching vibration (carboxylic acid groups of MWCNT). The characteristic stretching vibration of the –C–C–C group was observed around 1100 cm^{-1} [16]. Moreover, the bands at 400-600 cm^{-1} attributed to the Fe(Ni)–O feature peaks [20].

Fig. 1 (e) illustrated the XRD spectra of M-MWCNT. The prominent peaks at a 2θ of 18.65° (111), 30.32° (220), 35.57° (311), 43.16° (400), 53.25° (422), 56.85° (511), 62.071° (440) and 73.43° (533) were corresponded to the $NiFe_2O_4$ NPs (JCPDS no. 54-0964) [8]. MWCNT characteristic peaks were indicated at 2θ=26.12° (002), and 40.85° (100), which were identical to Yu et al report [28]. According to X-ray data the average crystal sizes of the pure $NiFe_2O_4$ and M-MWCNT are 21.62 and 7.25 nm, respectively.

The magnetic hysteresis loops of $NiFe_2O_4$ NPs and M-MWCNT nanocomposite were depicted in Fig. 1(f). Low remnant magnetization and coercivity in two specimens validated the superparamagnetic behavior, and the magnetic saturation value M_s is 28 and 7 emu/g for $NiFe_2O_4$ NPs and M-MWCNT,

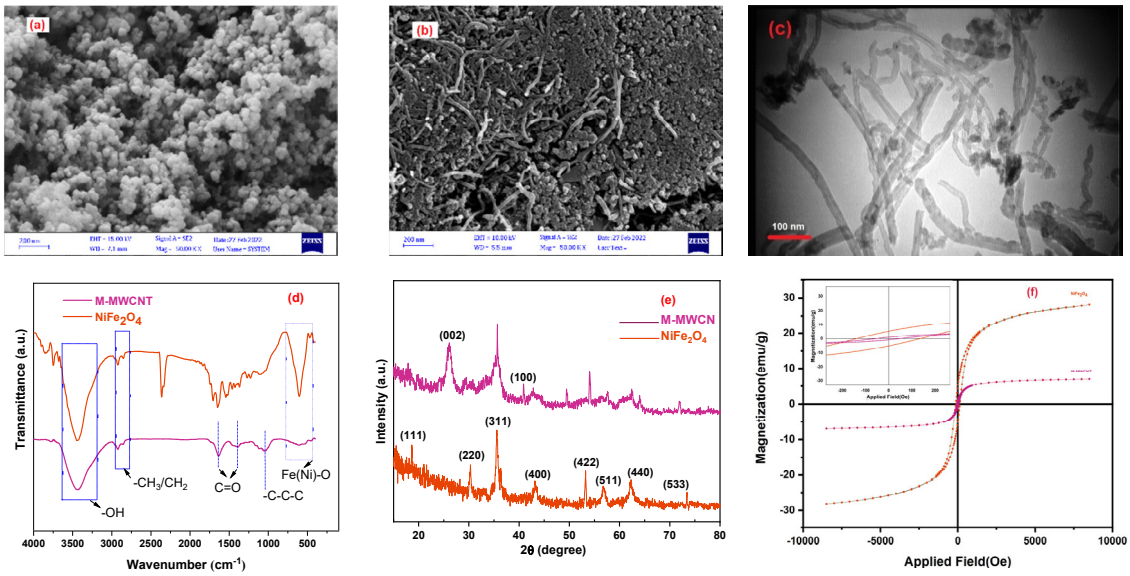

Fig. 1. Characterization of samples: SEM image of $NiFe_2O_4$ (a) and SEM image of M-MWCNTs (b), TEM image of M-MWCNTs (c), FTIR spectra (d), XRD spectrum (e), and magnetic hysteresis loop of samples (f).

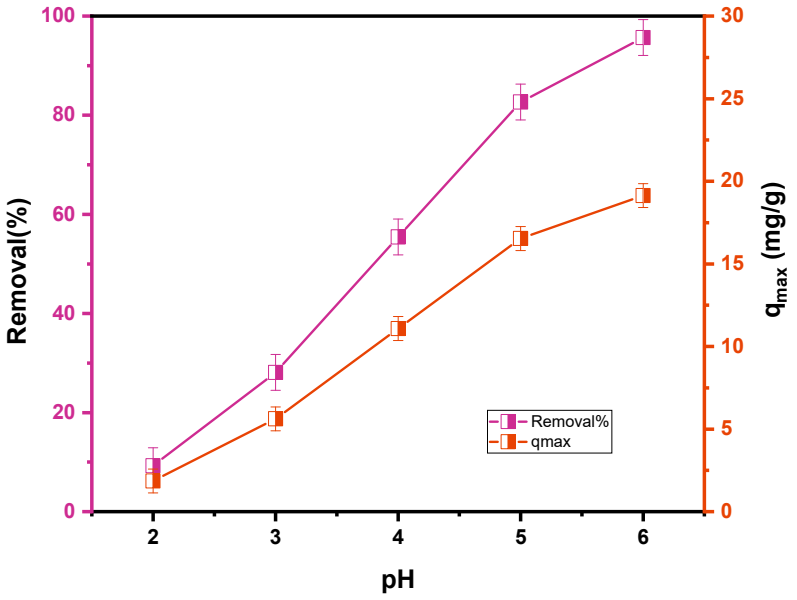

Fig. 2. Influence of pH magnitude for the removal and sorption capacity of Pb(II) onto M-MWCNT.

respectively. These data verified that the foreseen M-MWCNT was synthesized successfully [8].

Effect of pH

The pH magnitude impacts the charge transfer on the liquid/solid interface which influences the removal performance. Fig. 2 displayed outcomes of the experimentation at various pH magnitudes. In this work, the first reasons leading to Pb(II) sorption was the coordination reaction between –COOH and Pb(II). It was found that the lead is capable to reacts with –COOH and releasing H^+. Subsequently, it can be deduced that the removal performance of lead was confined via magnitude of pH. An increase in H^+ concentration has an unfavorable effect on the supersedence of the

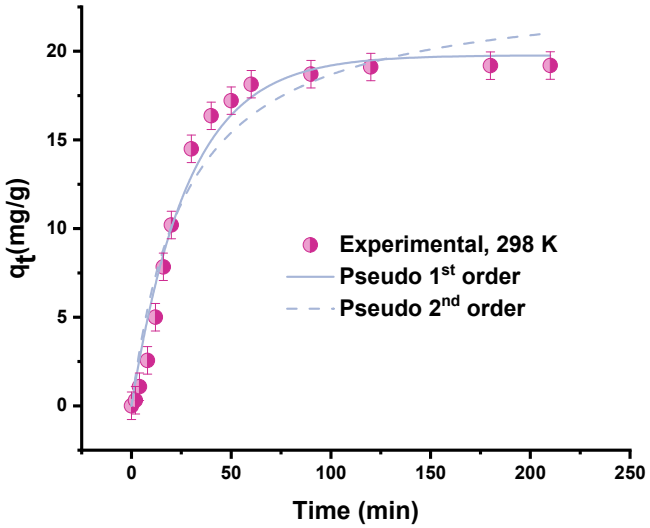

Fig. 3. Lagergren 1st order and pseudo 2nd order kinetics curve for Pb(II) onto M-MWCNTs.

Table 1. Kinetic parameters for Pb(II) adsorption onto M-MWCNTs.

Kinetic model	Parameters	Ion concentration (ppm)
		Pb(II)
		50
Pseudo 1st order	K_1 (1/min)	0.0353
	$q_{e,cal}$ (mg/g)	19.77
	R^2	0.9752
Pseudo 2nd order	K_2 (g/mg min)	0.0015
	$q_{e,cal}$ (mg/g)	23.72
	R^2	0.9472

H^+ from –COOH by lead ions. At low pH values, positive trend of replacement may be harshly limited [25]. Hence, a decrease in pH will be led to a decrease in the Pb(II) removal efficiency. Fig. 2 shows the highest amount of 95.7% in the solution with a pH of 5.5. Also, pH values higher than 6.0 was disbenefit to the Pb(II) removal efficiency, owing to the fact that the by-products of Pb like $Pb_4(OH)_4^{4+}$, $Pb_3(OH)_4^{2+}$ and $Pb(OH)^+$, were formed [29].

Kinetics of adsorption

A non-linear version of the Lagergren 1st order (LFO) and pseudo 2nd order (PSO) kinetic models was executed, as illustrated in Fig. 3, and estimated values of q_e, k_1, k_2, and R^2 are summarized in Table 1.

The Pb(II) kinetic upshots revealed that the LFO and PSO models both fitted the empirical data well. Furthermore, correlation coefficients (R^2) were reported 0.9755 and 0.9472 for LFO and PSO kinetics, respectively. This revealed that the LFO kinetic is the best model for sorption of Pb onto M-MWCNTs. As presented in Table 1, the q_e values achieved from LFO and PSO model were 19.77 and 23.72 mg/g, respectively.

Sorption isotherm

Freundlich and Langmuir are two basic models for the investigation of equilibrium sorption isotherms. According to Langmuir's theory, monolayer sorption occurs, while the Freundlich sorption isotherm is a benefit equation to express the sorption behavior on a heterogeneous surface [6]. Fig. 4 illustrates the amount of Pb(II) adsorbed on M-MWCNTs as a function of the equilibrium lead ion concentration. The related nonlinear constants and the calculated regression coefficients (R2) are tabulated in Table 2.

The Langmuir model provided much higher R2 magnitude (R2=0.9972) than did the Freundlich model for the lead ions sorption onto M-MWCNTs

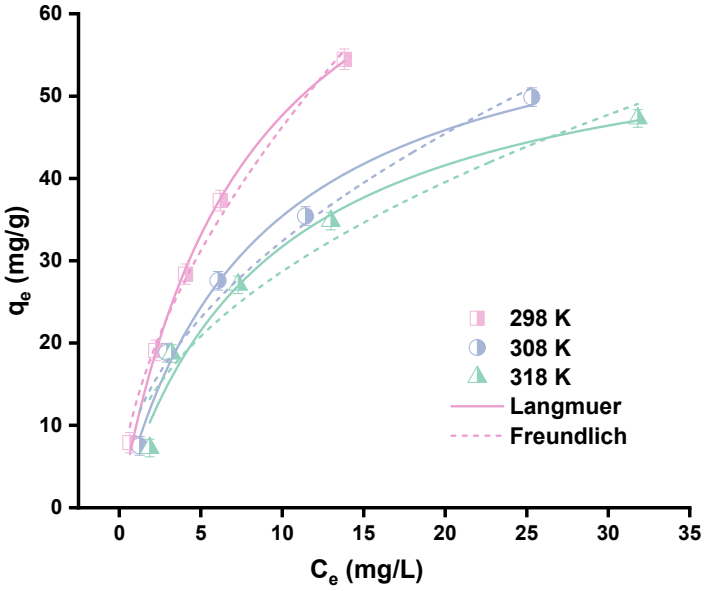

Fig. 4. Langmuir (a), and Freundlich (b) adsorption isotherms for Pb(II) onto M-MWCNTs.

Table 2. Isotherm factors for Pb(II) sorption onto M-MWCNTs.

Isotherm Parameters	Temperature (K)		
	DR16		
	298 K	308 K	318 K
Langmuir			
q_m (mg/g)	85.12	65.09	60.41
K_L (L/g)	0.1272	0.1193	0.1104
R^2	0.9972	0.9865	0.9732
Freundlich			
K_F (L/g)	12.512	10.486	9.8750
n	1.760	2.042	2.158
R^2	0.9896	0.9667	0.9245

Table 3. Comparison of Pb(II) adsorption on the different adsorbents.

Materials	Langmuir Adsorption Capacity (mg/g)	Rate constant (g/mg min)	Reference
ACMA	1.634	0.012	[30]
TC-AC	47.17	0.0205	[31]
TT-AC	46.95	0.0610	
SH-ATP	65.57	0.0136	[32]
CNTs/GP	52.74	0.0008	[33]
M-MWCNT	85.12	0.0015	Present Study

nanocomposite, showing its better fit with the empirical data. The value of Forster ¨ constant ($1<n<10$) in the Freundlich equation explains favorable sorption of Pb(II). As the n values of M-MWCNTs were in the favorable range (n =1.760, 2.042, and 2.158), shows that the sorption process of M-MWCNTs for Pb(II) is favorable sorption. The adsorption capacity of M-MWCNTs is compared with those obtained for other materials for Pb(II) and summarised in Table 3.

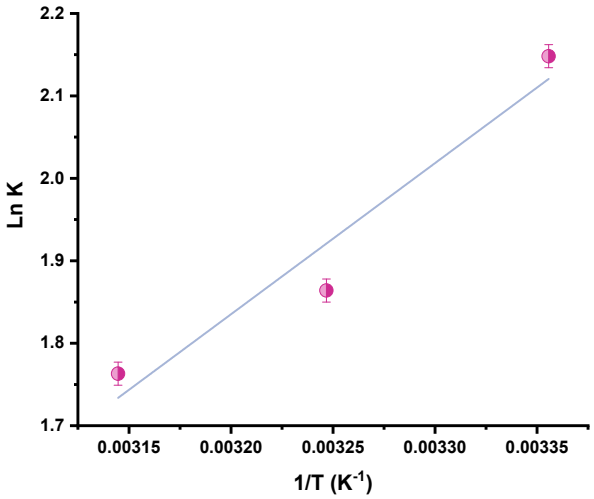

Fig. 5. Pattern of ln K_c vs. 1/*T* for Pb(II) sorption onto M-MWCNTs.

Table 4. Thermodynamic parameters for the sorption of Pb(II) on M-MWCNTs.

C_0 (mg/g)	Temperature (K)	$\Delta G°(KJ/mol)$	$\Delta S°(J/mol)$	$\Delta H°(KJ/mol)$
50	298	-5.322	-33.507	-15.239
	308	-4.773		
	318	-4.661		

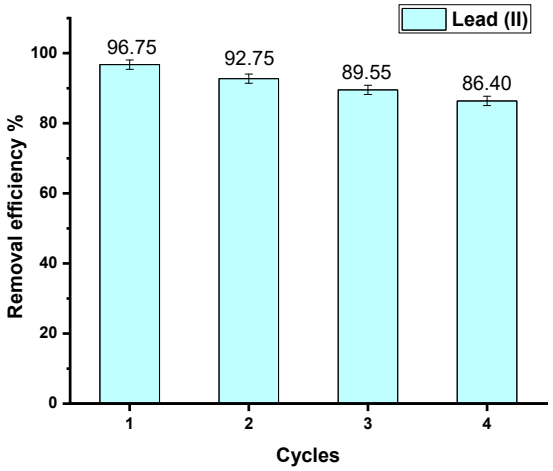

Fig. 6. Removal efficiency of M-MWCNT for Pb(II) after four successive sorption-desorption cycles.

Thermodynamic study

The ΔH° and ΔS° values can be achieved from the slope and intercept of Van't Hoff curve of Ln K_c vs. 1/T, respectively (Fig. 5). The negative value ΔH° reveals the exothermic nature of Pb(II) sorption on the M-MWCNT. Table 4 indicates the negative values of ΔG°, which confirmed that Pb(II) sorption on the M-MWCNT was spontaneous. Also, the negative value of ΔS° validates the decreased randomness at the solid/solute interface of Pb(II) on the M-MWCNT nanocomposites. Magnitudes of ΔG° are obtained close by 5 kJ/mol; this supports the verification that the sorption mechanism pursues the physisorption mechanism. Typically, it is proven that the ΔH° values in ranging from 2.1-20.9 kJ/mol imply a physisorption mechanism, while the chemisorption mechanism happens within 80 to 200 kJ/mol [21].

Desorption and reuses

In this work, the regeneration of M-MWCNT was investigated by 4 cycles of sorption/desorption. As shown in Fig. 6, the removal efficiency of Pb(II) decreases with the increase of cycle numbers. This phenomenon may be due to the active sites being occupied by metal ions and possible impurities. In the fourth regeneration cycle, the removal efficiency of Pb(II) onto M-MWCNT was 86.4%, which is 96.75% of the original removal efficiency. Moreover, this decline in the percentage probably could appear to be due to the loss of materials in the course of treatment/wash cycles.

CONCLUSION

The M-MWCNT nanoadsorbent synthesized by hydrothermal method and applied for Pb(II) sorption from wastewater. The characterization of the prepared M-MWCNT verified the successful fabrication of the metallic NPs with spherical shape in the nanocomposite. $NiFe_2O_4$ NPs are decorated on the outer walls of MWCNTs using covalent modified. Low remnant magnetization and coercivity in two specimens validated the superparamagnetic behavior. The size of $NiFe_2O_4$ nanoparticles in the structure of MWCNT was ~ 20 nm.The maximum adsorption capacity of M-MWCNT adsorbent reached 85.12 mg/g at 298 ºK and initial pH=5.5. Data illustrated that the Langmuir isotherm (R^2=0.9972) provided better description of Pb(II) adsorption, while LFO model (R^2=0.9752) fitted better than PFO kinetic model. Thermodynamic studies showed the exothermic sorption process and suggest physisorption as the dominant reaction governing lead sorption by nanocomposite. Further, M-MWCNT adsorbent also possesses a good reusability (4 cycles) for Pb(II) removal.

ACKNOWLEDGMENT

The authors gratefully acknowledge Neyshabur Branch, Islamic Azad University, Neyshabur, Iran.

CONFLICTS OF INTEREST

The authors do not have any conflicts of interest.

REFERENCES

[1] Abdollahi B., Salari D., Zarei M., (2022), Synthesis and characterization of magnetic Fe_3O_4@ SiO_2-MIL-53 (Fe) metal-organic framework and its application for efficient removal of arsenate from surface and groundwater. *J. Env. Chem. Eng.* 10: 107144-107148.

[2] Kończyk J., Żarska S., Ciesielski W., (2019), Adsorptive removal of Pb (II) ions from aqueous solutions by multi-walled carbon nanotubes functionalised by selenophosphoryl groups: Kinetic, mechanism, and thermodynamic studies. *Colloids and Surf. A: Physicochem. Eng. Asp.* 575: 271-282.

[3] Awual M. R., Hasan M. M., Islam A., Rahman M. M., Asiri A. M., Khaleque M. A., Sheikh M. C., (2019), Offering an innovative composited material for effective lead (II) monitoring and removal from polluted water. *J. Cleaner Prod.* 231: 214-223.

[4] Abdel-Ghani N., Hefny M., El-Chaghaby G. A., (2007), Removal of lead from aqueous solution using low cost abundantly available adsorbents. *Int. J. Env. Sci. Technol.* 4: 67-73.

[5] Zhang K., Gao X., Zhang Q., Li T., Chen H., Chen X., (2017), Synthesis, characterization and electromagnetic wave absorption properties of asphalt carbon coated graphene/ magnetic $NiFe_2O_4$ modified multi-wall carbon nanotube composites. *J. Alloys & Comp.* 721: 268-275.

[6] Zhao W., Tian Y., Chu X., Cui L., Zhang H., Li M., Zhao P., (2021), Preparation and characteristics of a magnetic carbon nanotube adsorbent: Its efficient adsorption and recoverable performances. *Separ. Purif. Technol.* 257: 117917-117921.

[7] Zhou L., Ji L., Ma P.-C., Shao Y., Zhang H., Gao W., Li Y., (2014), Development of carbon nanotubes/$CoFe_2O_4$ magnetic hybrid material for removal of tetrabromobisphenol A and Pb (II). *J. Hazard. Mater.* 265: 104-114.

[8] Jiang R., Zhu H.-Y., Fu Y.-Q., Zong E.-M., Jiang S.-T., Li J.-B., Zhu J.-Q., Zhu Y.-Y., (2021), Magnetic $NiFe_2O_4$/MWCNTs functionalized cellulose bioadsorbent with enhanced adsorption property and rapid separation. *Carbohyd. Polym.* 252: 117158-117162.

[9] Luo X., Lei X., Cai N., Xie X., Xue Y., Yu F., (2016), Removal of heavy metal ions from water by magnetic cellulose-based beads with embedded chemically modified magnetite nanoparticles and activated carbon. *ACS Sustain. Chem. Eng.* 4: 3960-3969.

[10] Ren L., Lin H., Meng F., Zhang F., (2019), One-step solvothermal synthesis of Fe_3O_4@ Carbon composites and their application in removing of Cr (VI) and Congo red. *Ceram. Int.* 45: 9646-9652.

[11] Wang N., Ouyang X.-K., Yang L.-Y., Omer A. M., (2017), Fabrication of a magnetic cellulose nanocrystal/metal–organic framework composite for removal of Pb (II) from water. *ACS Sustain. Chem. Eng.* 5: 10447-10458.

[12] Aslibeiki B., Eskandarzadeh N., Jalili H., Varzaneh A. G., Kameli P., Orue I., Chernenko V., Hajalilou A., Ferreira L., Cruz M., (2022), Magnetic hyperthermia properties of $CoFe_2O_4$ nanoparticles: Effect of polymer coating and interparticle interactions. *Ceram. Int.* In Press.

[13] Hakimyfard A., Khademinia S., (2022), Hirshfeld surface analysis of solid-state synthesized $NiFe_2O_4$ nanocomposite and application of it for photocatalytic degradation of Water pollutant dye. *Int. J. Nano Dimens.* 13: 155-167.

[14] Bagheri Gh. A., Ashayeri V., Mahanpoor K., (2013), Photocatalytic efficiency of $CuFe_2O_4$ for photodegradation of acid red 206. *Int. J. Nano Dimens.* 4: 111-115.

[15] Abideen Idowu A., Sarafadeen Olateju K., Oluwatobi Samson A., (2019), Synthesis of $MnFe_2O_4$ nanoparticles for adsorption of digestive enzymes: Kinetics, isothermal and thermodynamics studies. *Int. J. Nano Dimens.* 10: 330-339.

[16] Ensafi A. A., Allafchian A. R., Rezaei B., Mohammadzadeh

R., (2013), Characterization of carbon nanotubes decorated with $NiFe_2O_4$ magnetic nanoparticles as a novel electrochemical sensor: Application for highly selective determination of sotalol using voltammetry. *Mater. Sci. Eng.: C.* 33: 202-208.

[17] Kafshgari L. A., Ghorbani M., Azizi A., (2017), Fabrication and investigation of $MnFe_2O_4$/MWCNTs nanocomposite by hydrothermal technique and adsorption of cationic and anionic dyes. *Appl. Surf. Sci.* 419: 70-83.

[18] Foroutan R., Peighambardoust S. J., Esvandi Z., Khatooni H., Ramavandi B., (2021), Evaluation of two cationic dyes removal from aqueous environments using CNT/MgO/$CuFe_2O_4$ magnetic composite powder: A comparative study. *J. Env. Chem. Eng.* 9: 104752-104757.

[19] Sadegh H. R., Shahriary Ghoshehkandi R., Masjedi A., Mahmoodi Z., Kazemi M., (2016), A review on Carbon nanotubes adsorbents for the removal of pollutants from aqueous solutions. *Int. J. Nano Dimens.* 7: 109-120.

[20] Hazarika M., Chinnamuthu P., Borah J., (2022), Enhanced photocatalytic efficiency of MWCNT/$NiFe_2O_4$ nanocomposites. *Phys. E: Low-dimens. Sys. Nanostruc.* 139: 115177-115182.

[21] Forghani M., Azizi A., Livani M. J., Kafshgari L. A., (2020), Adsorption of lead (II) and chromium (VI) from aqueous environment onto metal-organic framework MIL-100 (Fe): Synthesis, kinetics, equilibrium and thermodynamics. *J. Solid State Chem.* 291: 121636-121641.

[22] Powell K. J., Brown P. L., Byrne R. H., Gajda T., Hefter G., Leuz A.-K., Sjöberg S., Wanner H., (2009), Chemical speciation of environmentally significant metals with inorganic ligands. Part 3: The Pb^{2+} , OH^-, Cl^-, CO_3^{2-}, SO_4^{2-}, and PO_4^{3-}systems (IUPAC Technical Report). *Pure and Appl. Chem.* 81: 2425-2476.

[23] Sylva R. N., Brown P. L., (1980), The hydrolysis of metal ions. Part 3. Lead (II). *J. Chem. Soc. Dalton Transactions*. 1577-1581.

[24] Breza M., Manová A., (2002), On the structure of Lead (II) complexes in aqueous solutions. III. Hexanuclear clusters. *Collec. Czechoslovak Chem. Communic.* 67: 219-227.

[25] Lian Q., Ahmad Z. U., Gang D. D., Zappi M. E., Fortela D. L. B., Hernandez R., (2020), The effects of carbon disulfide driven functionalization on graphene oxide for enhanced Pb (II) adsorption: Investigation of adsorption mechanism. *Chemosphere*. 248: 126078-126082.

[26] Mondal S. K., Welz A., Rezaei F., Kumar A., Okoronkwo M. U., (2020), Structure–property relationship of geopolymers for aqueous Pb removal. *ACS Omega.* 5: 21689-21699.

[27] Das A., Bar N., Das S., (2022), Adsorptive removal of Pb (II) ion on arachis hypogaea's shell: Batch experiments, statistical, and GA modeling. *Int. J. Env. Sci. Technol.* 1-14.

[28] Yu X., Wang D., Yuan B., Song L., Hu Y., (2016), The effect of carbon nanotubes/$NiFe_2O_4$ on the thermal stability, combustion behavior and mechanical properties of unsaturated polyester resin. *RSC Adv.* 6: 96974-96983.

[29] Qu G., Zhou J., Liang S., Li Y., Ning P., Pan K., Ji W., Tang H., (2022), Thiol-functionalized multi-walled carbon nanotubes for effective removal of Pb (II) from aqueous solutions. *Mater. Chem. Phys*. 278: 125688-125692.

[30] Neolaka Y. A., Lawa Y., Naat J., Riwu A. A., Darmokoesoemo H., Widyaningrum B. A., Iqbal M., Kusuma H. S., (2021), Indonesian kesambi wood (Schleichera oleosa) activated with pyrolysis and H_2SO_4 combination methods to produce mesoporous activated carbon for Pb(II) adsorption from aqueous solution. *Env. Technol. Innovat.* 24: 101997-102002.

[31] Eletta O. A., Ayandele F. O., Ighalo J. O., (2021), Adsorption of Pb(II) and Fe(II) by mesoporous composite activated carbon from Tithonia diversifolia stalk and Theobroma cacao pod. *Biomass Convers. Bioref.* 1-10.

[32] Fu C., Zhu X., Dong X., Zhao P., Wang Z., (2021), Study of adsorption property and mechanism of lead (II) and cadmium (II) onto sulfhydryl modified attapulgite. *Arab. J. Chem.* 14: 102960-102966.

[33] Yan S., Ren X., Zhang F., Huang K., Feng X., Xing P., (2022), Comparative study of Pb^{2+}, Ni^{2+}, and methylene blue adsorption on spherical waste solid-based geopolymer adsorbents enhanced with carbon nanotubes. *Separ. Purif. Technol.* 284: 120234-120239.